HHS Public Access

Author manuscript

Neuroscience. Author manuscript; available in PMC 2017 September 07.

Published in final edited form as:

Neuroscience. 2016 September 07; 331: 1–12. doi:10.1016/j.neuroscience.2016.06.010.

STATUS EPILEPTICUS STIMULATES NDEL1 EXPRESSION VIA THE CREB/CRE PATHWAY IN THE ADULT MOUSE BRAIN

YUN-SIK CHOI[a], **BOYOUNG LEE**[b], **KATELIN F. HANSEN**[c], **SYDNEY ATEN**[c], **PAUL HORNING**[c], **KELIN L. WHEATON**[d], **SOREN IMPEY**[e], **KARI R. HOYT**[d], and **KARL OBRIETAN**[c,*]

[a]Department of Pharmaceutical Science & Technology, Catholic University of Daegu, Gyeongbuk, Republic of Korea

[b]Center for Cognition and Sociality, Institute for Basic Science, Seoul, Republic of Korea

[c]Department of Neuroscience, Ohio State University, Columbus, OH, USA

[d]Division of Pharmacology, Ohio State University, Columbus, OH, USA

[e]Oregon Health and Science University, Portland, OR, USA

Abstract

Nuclear distribution element-like 1 (NDEL1/NUDEL) is a mammalian homolog of the *Aspergillus nidulans* nuclear distribution molecule NudE. NDEL1 plays a critical role in neuronal migration, neurite outgrowth and neuronal positioning during brain development; however within the adult central nervous system, limited information is available regarding NDEL1 expression and functions. Here, the goal was to examine inducible NDEL1 expression in the adult mouse forebrain. Immunolabeling revealed NDEL1 within the forebrain, including the cortex and hippocampus, as well as the midbrain and hypothalamus. Expression was principally localized to perikarya. Using a combination of immunolabeling and RNA seq profiling, we detected a marked and long-lasting upregulation of NDEL1 expression within the hippocampus following a pilocarpine-evoked repetitive seizure paradigm. Chromatin immunoprecipitation (ChIP) analysis identified a cAMP response element-binding protein (CREB) binding site within the CpG island proximal to the *NDEL1* gene, and *in vivo* transgenic repression of CREB led to a marked downregulation of seizure-evoked NDEL1 expression. Together these data indicate that NDEL1 is inducibly expressed in the adult nervous system, and that signaling via the CREB/CRE transcriptional pathway is likely involved. The role of NDEL1 in neuronal migration and neurite outgrowth during development raises the interesting prospect that inducible NDEL1 in the mature nervous system could contribute to the well-characterized structural and functional plasticity resulting from repetitive seizure activity.

Keywords

seizure; CREB; CRE; hippocampus; NDEL1

[*]Corresponding author. Address: K. Obrietan, Department of Neuroscience, Ohio State University, Graves Hall, Room 4118, 333 West 10th Avenue, Columbus, OH 43210, USA. Tel: +1-(614)-292-4432; fax: +1-(614)-688-8742. obrietan.1@osu.edu (K. Obrietan).

INTRODUCTION

Nuclear distribution element-like 1 (NDEL1/NUDEL) is a mammalian homolog of the nuclear distribution molecule NudE. NDEL1 is broadly expressed, with particularly high levels detected in the brain. NDEL1 interacts with a number of proteins, including dynein, lissencephaly 1 protein (LIS1), disrupted in schizophrenia 1 (DISC1), and 14-3-3ζ (Chansard et al., 2011; Vallee et al., 2012; Bradshaw et al., 2013). Through its interactions with LIS1, and as part of the dynein motor complex, NDEL1 has been shown to play a variety of roles in cytoskeletal organization throughout development. Along these lines, in progenitor cell populations, NDEL1 is concentrated at the centrosome and regulates mitotic spindle pole organization and mitosis (Guo et al., 2006; Moon et al., 2014); whereas in developing postmitotic neurons, NDEL1 redistributes to axons and cell soma and is essential for normal neuronal migration, cortical layering, neurite outgrowth and neuronal polarity (Niethammer et al., 2000; Sasaki et al., 2000; Lambert de Rouvroit and Goffinet, 2001; Toyo-oka et al., 2003; Kamiya et al., 2006; Youn et al., 2009). Consistent with these key developmental processes, germline deletion of NDEL1 is embryonically lethal at the peri-implantation stage (Sasaki et al., 2005).

In the adult central nervous system NDEL1 was found to interact with neurofilament light subunit (NF-L) and to facilitate the polymerization of NFs (Sasaki et al., 2000; Nguyen et al., 2004). Further, the deletion of NDEL1 in the postnatal mouse brain causes NF alterations reminiscent of those observed during neurodegeneration (Nguyen et al., 2004), thus indicating a key role for NDEL1 in neuronal morphology. Additional functional roles for NDEL1 in the soma and cell processes include lysosome transport and organelle positioning (Zhang et al., 2009; Lam et al., 2010). Notably, dysregulation of NDEL1 has been linked to an array of mental and neurodegenerative disorders (Chansard et al., 2011). For example, through its interactions with LIS1 and DISC1, NDEL1 may contribute to the etiology of lissencephaly and schizophrenia, respectively (Ozeki et al., 2003; Shu et al., 2004; Kamiya et al., 2006; Youn et al., 2009).

Although these studies have revealed functional aspects of NDEL1 in the mature brain, there is still limited information about its neuroanatomical expression and whether NDEL1 is regulated in an activity-dependent manner. Considering the dynamic roles of NDEL1 in transport, neurite outgrowth and the integrity of adult CNS neurons, we posited that NDEL1 may be important for synaptic modification and reorganization following pathophysiological levels of neuronal activity. Here, we begin to address this question with a series of immunolabeling, ChiP Seq, RNA profiling and transgene studies. The findings presented here reveal that NDEL1 expression is regulated by neuronal activity in the mature CNS and that its expression is under the control of the CREB/CRE transcriptional pathway.

EXPERIMENTAL PROCEDURES

Animals and tissue processing

C57BL/6 mice (mixed gender: 7–10 weeks of age) were used for all of the experiments described here. A total of 52 mice were used to generate the data presented in Figs. 1–3 and 6; data presented in Figs. 4 and 5B were curated from our recently published Illumina

Sequencing studies (Lesiak et al., 2013; Hansen et al., 2014); data presented in Fig. 5A was derived from a combination of *in silico* studies and cell culture studies published as part of the ENCODE consortium project (for additional details, please see the ChIP seq section below). For immunolabeling assays, mice were anesthetized with an intraperitoneal injection of ketamine (91 mg/ml) and xylaxine (9 mg/ml) and then transcardially perfused with cold saline, followed by 4% paraformaldehyde in phosphate-buffered saline (PBS, pH 7.4). Brains were then post-fixed in 4% paraformaldehyde for 4 h at 4 °C and cryoprotected with 30% sucrose solution in PBS. Coronal sections (40 μm) through the whole brain were prepared using a freezing microtome. For Western analysis, mice were euthanized via CO_2 – mediated asphyxiation, brains were isolated and placed in ice-cold oxygenation media, and the striatum were rapidly dissected and stored at −80 °C. A detailed description of the tissue isolation method for the RNA seq analysis is provided in Hansen et al. (2014). All procedures involving mice were approved by the Institutional Animal Care and Use Committee at Ohio State University.

Immunohistochemistry and immunofluorescence

For immunohistochemistry, sections were washed with phosphate-buffered saline (PBS) and incubated in 0.3% hydrogen peroxide/PBS for 20 min to eliminate endogenous peroxidase-like activity. After several washes with PBS, sections were blocked with 10% normal goat serum in PBS, followed by overnight incubation with rabbit anti-NDEL1 antibody (1:1000 dilution: Life Technologies, # PA5-19996, Carlsbad, CA, USA) at 4 °C. Sections were then processed using the ABC staining method (Vector Lab, Burlingame, CA, USA). Nickel-intensified diaminobenzidine (DAB: Vector Labs) was used to visualize the signal. To demonstrate the specificity of anti-NDEL1 antibody, synthetic NDEL1 peptide (Zymed laboratories) was mixed with anti-NDEL1antibody (1:100 excess of the peptide) and incubated for 5 min at room temperature just before the tissues were labeled using the noted procedures. Photomicrographs were captured using a 16-bit digital camera (Micromax YHS 1300; Princeton Instruments, Trenton, NJ. USA) mounted on a Leica DM IRB microscope (Nussloch, Germany).

For immunofluorescence labeling, sections were washed in PBS with 0.1% Triton-X (PBST), and then incubated with PBST containing 0.3% hydrogen peroxide with 10% normal goat serum in PBS (40 min). Next, tissue was incubated overnight with both rabbit anti-NDEL1 (1:100 dilution: Life Technologies) and one of the following antibodies: mouse anti-glial fibrillary acidic protein (GFAP) (1:250 dilution; Invitrogen #A21282, Waltham, Massachusetts, USA); mouse anti-parvalbumin (1:250 dilution; Chemicon #MAB1572, Temecula, CA, USA); chicken anti-green fluorescent protein (GFP) (1:2000 dilution; Abcam #: ab13970, Cambridge UK).

To develop a fluorescence signal for NDEL1, we utilized the tyramide amplification method described by Vize et al. (2009). To this end, sections were labeled with a goat anti-rabbit horseradish peroxidase-conjugated secondary antibody (1:500 dilution; Perkin Elmer, Waltham, MA, # NEF812001EA) for 2 h at room temperature in PBS containing 10% normal goat serum. Next, sections were incubated with tyramide Alexa 488 substrate in PBS containing 10 mM imidazole, 0.2% bovine serum albumin, 0.0015% hydrogen peroxide, and

0.05% Tween 20 for 1 h. Following the tyramide labeling sections were washed and standard labeling for the second primary antibody was performed. To this end, sections were incubated with Alexa 594-conjugated secondary antibodies (1:1000; Molecular Probes, Eugene, OR, USA) to either mouse IgG (for the GFAP and parvalbumin primary antibodies) or chicken IgG (for the GFP primary antibody) for 2 h at room temperature. Lastly, sections were labeled with the DNA stain DraQ5 (Biostatus Limited, 1:5000 dilution, Leicestershire, UK) then mounted with Gelmount (Biomeda, Hatfield, PA, USA). Images were captured using a Zeiss 510 Meta confocal microscope (2-μm-thick optical section).

Ratiometric densitometric analysis was used to quantify NDEL1 expression. To this end, fluorescence photomicrographs of NDEL1 expression were captured using a Leica DMIRB microscope at 20× magnification and images were acquired and quantitation was performed using MetaMorph software (Universal Imaging, West Chester, PA). Forty-μm regions of the GCL (upper and lower blades), the lateral CA3 and the medial CA1 were outlined and the mean labeling intensity was determined using a 0–255 unit, 8-bit scale. On a section-by-section basis, ratiometric values were generated by dividing the intensity values of the noted regions with the NDEL1 labeling values within the corpus callosum; of note, NDEL1 expression within the corpus callosum was not significantly different between wildtype (WT) and A-CREB transgenic mice. Regions were collected from two dorsal hippocampal sections, per animal; sections were separated by an ~200-μm interval (stereotaxic coordinate AP, approximately −1.30 mm to −2.00 mm). Ratiometric data were averaged for each animal and the mean value (plus the standard error of the mean) of each group is presented. Significance was assessed using a two-tailed Student's *t*-test.

Fluoro-Jade labeling

Formaldehyde-fixed thin-brain sections were prepared as described above, mounted on gelatin-coated slides, washed with distilled water, and then immersed in a solution of 0.2% NaOH/80% ethanol (5 min). Next, the slides were transferred to 70% ethanol solution (2 min), rinsed with distilled water (2 min) and then immersed in a 0.06% potassium permanganate solution (5 min). Slides were then incubated in solution of 0.00015% Fluoro-Jade C and 0.1% acetic acid (20 min). After washing in distilled water, the sections were dried, cleared with xylenes (3 min) and coverslipped with DPX mounting media. A total of 16 mice were used for our Fluro-Jade data sets.

Western blotting

Striatal tissue was suspended and sonicated in RIPA buffer (50 mM Tris–HCl, 1% NP-40, 0.25% Na-deoxycholate, 150 mM NaCl, 1 mM EDTA, 1 mM sodium vanadate and 1 mM NaF-containing protease inhibitor cocktail: Roche Bio.) and supernatants were isolated by centrifugation (13,000×*g*) for 10 min. Immediately prior to loading, lysates (5 μg/lane) were diluted in 6× gel-loading buffer, then electrophoresed on a 12% SDS polyacrylamide gel. Samples were transblotted onto polyvinylidene fluoride membrane (Immobilon P; Millipore, Bedford, MA, USA), blocked, and then incubated with the noted NDEL1 antibody (Life Technologies, 1:2,000), Membranes were then washed and incubated (2 h at room temperature) with horseradish peroxidase-conjugated secondary antibody (1:2,000; PerkinElmer Life Sciences, Norwalk, CT, USA), and the signal was visualized by using

Renaissance Chemiluminescent HRP substrate (PerkinElmer Life Sciences). Subsequently, the blots were stripped and labeled with rabbit p44/42 antibody (Santa Cruz, 1:2000, Dallas, TX, USA) and then rabbit anti-eGFP antibody (1:4,000, Clontech, Mountain View, CA, USA) and labeling was visualized as described above. Image J software was used to quantitate band intensity. Band intensity for NDEL1 was normalized to the ERK1 level for the corresponding lane. Data were averaged for each condition and the mean value (plus the standard error of the mean) for each group is presented. Analysis was performed on lysates from 6 animals: three for each condition. Datasets were confirmed using a second cohort of mice; 6 animals: three for each condition. Significance was assessed using a two-tailed Student's *t*-test.

Pilocarpine-induced status epilepticus (SE), and tissue profiling

Animals initially received an intraperitoneal (i.p.) injection with 1 mg/kg atropine methyl nitrate (Sigma) 30 min before being injected (i.p.) with pilocarpine (325 mg/kg, Sigma, diluted in physiological saline,). SE was defined as a continuous (>60 min) motor seizure of stage 4 (rearing and falling), 5 (loss of balance, continuous rearing and falling) or stage 6 (severe tonic–clonic seizures). Only mice that developed SE after pilocarpine administration were used. For experiments involving A-CREB transgenic mice (and their non-transgenic counterparts) SE was terminated after 2 h with diazepam (5 mg/kg, i.p.); for all other experiments, SE was not terminated. Both A-CREB transgenic and WT mice exhibited robust seizure activity, with both lines exhibiting approximately 40% mortality at 1 day post-SE. For immunohistochemical processing, mice were sacrificed 6 h, 2 days or 4 weeks post-SE using the methods described above. A total of 16 animals (4 animals per time point) were used for this analysis. The RNA deep sequencing on NDEL1 data was generated as part of our recent work examining SE-evoked gene expression (Hansen et al., 2014). As such, the details of the tissue isolation method, RNA purification, and all sequence profiling and analysis steps can be found in Hansen et al. (2014). Briefly, expression of *NDEL1* at each of the 3 post-SE time points (12 h, 2 days, 6 weeks) was analyzed in relation to NDEL1 expression under the control (no stimulation) condition. For this, analysis, likelihood-ratio statistic (Marioni et al., 2008) and the Storey *Q*-test were performed to correct for multiple comparisons (Bioconductor *q* value package). Ref-Seq genes with a *q* value <0.01 were considered significant. Here, only the 12-h time point reached significance. The RNA seq data from the Hansen et al. (2014) study can be viewed via the NCBI database GEO (http://www.ncbi.nlm.nih.gov/geo/) using the following accession code: GSE72402.

A-CREB transgenic mice

A description of the generation of the tetracycline-inducible bicistronic A-CREB-eGFP transgenic mouse strain can be found in Lee et al. (2007). To drive transgene expression, the A-CREB-eGFP mice were crossed with αCaMKII promoter-tTA transgenic mice (Mayford et al., 1996). Bitransgenic offspring were identified via PCR-based genotyping, and transgene expression was confirmed using immunohistochemistry against eGFP. A-CREB-eGFP:tTA mice (hereafter referred to as A-CREB mice) were maintained on a C57BL/6 background. Dynamic regulation of A-CREB via doxycycline was not used in any of the experiments described here. A total of 8 animals (4 of each genetype: A-CREB and wild-type) were used for this analysis.

ChIP seq

For the human NDEL1 gene, the 2009 (GRCh37/hg19) assembly was loaded onto the UCSC genome browser, and the ATF1, AFT3 and CREB ChIP tracks provided by the Encode Consortium and were uploaded under the ENCODE Regulation 'Super-track' setting. ATF1 ChIP data were generated using K562 cells (untreated, UCSC Accession: wgEncodeEH002865); ATF3 ChIP data were generated using K562 cells (untreated, UCSC Accession: wgEncodeEH001662); CREB1 ChIP data were generated using A549 cells (treated with dexamethasone, UCSC Accession: wgEncode EH001662). Details of the ChIP methods can be found in (http://genome.cshlp.org/content/22/9/1798.long). Murine CREB ChIP profiling data were derived from the published work of Lesiak et al. (2013). We used the blat option on the UCSC genome browser (MM9 2007 genome assembly) to generate the ChIP tag count data presented here. CpG island data were pulled-up as part of the UCSC browser, and were based on the CpG analysis methods described by (Gardiner-Garden and Frommer, 1987). For clarity, Genome Browser assembly data were reorganized in Photoshop, and unnecessary information was eliminated.

RESULTS

NDEL1 expression in the adult mouse brain

Initially, we performed an immunohistochemical analysis of NDEL1 expression in the adult mouse brain. As shown in Fig. 1, NDEL1 expression was detected in the motor cortex, striatum and the cerebellum (Fig. 1A–C). Scattered NDEL1-expressing cells were also observed in the hypothalamus, including the suprachiasmatic nucleus (Fig. 1D), periventricular nucleus and paraventricular nucleus (data not shown). The specificity of the antibody used for this study was tested by incubating it with a synthetic NDEL1 peptide prior to immunolabeling. With this approach, the noted NDEL1 expression pattern was eliminated: representative data are presented for the motor cortex (Fig. 1E). Further, Western analysis with the same NDEL1 antibody generated an ~38 kd band, which is consistent with the molecular mass of NDEL1 (Fig. 6).

Inducible NDEL1 expression

Next, we examined whether synaptic activity regulates NDEL1 expression. To this end we utilized the pilocarpine model of status epilepticus (SE) and examined induction within the hippocampus. Pilocarpine is a muscarinic acetylcholine receptor agonist that elicits a dose-dependent increase in synaptic discharges within the hippocampus, with high levels of pilocarpine leading to the development of SE. Of interest to us here, SE triggers a well characterized set of pathophysiological effects within the hippocampus, including the loss of hilar interneurons and pyramidal cells of the CA3 and CA1 cell layer, via both necrotic and apoptotic mechanisms (Fujikawa et al., 2000; Wang et al., 2008). Further, SE leads to robust granule cell synaptic reorganization and granule cell dispersion (Leite et al., 2002; Dudek et al., 2002). Given that NDEL1 is thought to play an important role in synaptic modification and in neuronal migration during development, we posited that SE, would be a suitable model system to examine inducible NDEL1 expression within the adult nervous system.

For our immunohistochemical analysis of NDEL1, mice were sacrificed 6 h, 2 days or 4 weeks after SE. In control mice (no pilocarpine) limited NDEL1 expression was detected in the hippocampus (Fig. 2A). In contrast to control mice, SE evoked a marked increase in NDEL1 expression at all three time points (Fig. 2A, B). Induction was detected in the principal cell layers (i.e., CA1, CA3 and GCL), and at a cellular level, this increase in labeling was observed in both the cell processes and in the perikarya (Fig. 2B). To confirm that our SE paradigm elicited the expected cell death profile, hippocampal tissue was isolated 2 days post-SE and processed using Fluoro-Jade, and marker of dead and dying cells. As expected, marked cell death was observed in the CA1 cell layer and in the hilus; with limited cell death detected in the granule cell layer (Fig. 2C).

Immunohistochemical analysis was complemented by double immunofluorescence labeling at the 2-day post-SE time point to identify NDEL1-positive cell populations in the hippocampus (Fig. 3A, B). As anticipated, double labeling with the neuronal marker protein NeuN (Fig. 3C, D), revealed robust increases in NDEL1 expression within the CA1 and granule cell layers. In addition, using parvalbumin A as a marker of GABAergic neurons, we also found SE-evoked NDEL1 expression in inhibitory neuronal populations (Fig. 3E); inducible NDEL1 expression was also detected in hilar interneuron cell populations (data not shown). However, in contrast with the noted findings, an SE-evoked increase in NDEL1 expression was not detected in glial cell populations, as assessed by double labeling for NDEL1 and GFAP (Fig. 3F); rather, within the glial cell population, NDEL1 expression was relatively low under both the control condition and at 2 days-post SE.

Consistent with the findings from the immunolabeling studies, data from our recently published RNA seq epileptogenesis study (Hansen et al., 2014) detected upregulation of NDEL1 from 12 h to 6 weeks post-SE (Fig. 4A, B). Here we provide both representative tag count data from the *NDEL1* locus (for the control condition and for 12 h post-SE: Fig. 4A) and fold-change tag count data over the 3 post-SE time points (Fig. 4B). Interestingly, the long-lasting upregulation of NDEL1 following SE parallels the time course required for robust synaptic reorganization within the hippocampus (Mathern et al., 1998). In total, these data reveal that NDEL1 is upregulated by repetitive seizure activity in the hippocampus, and that NDEL1 remained elevated throughout the period of robust structural remodeling.

CREB-mediated NDEL1 expression

The induction of NDEL1 following seizure activity led us to examine potential transcriptional control mechanisms. To this end, bioinformatic (*in silico*) analysis of the promoter/enhancer region of the human *NDEL1* gene detected a conserved cyclic AMP response element (CRE) motif within a CpG island (Fig. 5A), and ChIP seq data provided by the Encode Consortium revealed that the binding of ATF/CREB family members (i.e., ATF3, ATF1 and CREB) was associated with this CRE motif (Fig. 5A). The presence of a CRE site is notable, given that transcription via the CREB/CRE pathway is regulated by synaptic activity. Further, our data have shown that SE triggers a robust and persistent increase in CRE-mediated gene expression within the hippocampus (Lee et al., 2007 and Hansen et al., 2014). Similar to the human dataset, CREB ChIP seq data from mouse

neurons (Lesiak et al., 2013) detected robust CREB binding within the CpG island proximal to the majority of *NDEL1* gene variants (Fig. 5B).

Next, we tested the role of CREB in NDEL1 expression using our A-CREB transgenic mouse line (Lee et al., 2007). A-CREB potentially suppresses CREB-dependent transcription by binding to the basic leucine zipper region of endogenous CREB, and in turn inhibiting its ability to bind to the cAMP response element (Ahn et al., 1998). Our A-CREB construct was also engineered to drive the expression of an enhanced green fluorescent protein (eGFP) tag from an internal ribosomal entry site. As an initial assessment of the effects of CREB repression on NDEL1 expression, striatal lysates from A-CREB transgenic and WT mice were probed for NDEL1 expression via Western analysis. With this approach, we found that NDEL1 expression was significantly reduced in A-CREB transgenic mice, compared to WT controls (Fig. 6A; P=0.018, unpaired two-tailed Student's t-test, t=7.349, df=2; F test to compare variance did not reveal a significant difference between the two genotypes: P=0.2574, F=2.886, DFn=2, DFd=2). Next, SE-evoked NDEL1 expression within the hippocampus was profiled in A-CREB transgenic and WT mice. Given the high level of cell death associated with prolonged SE, and work reporting an elevated cell death profile from the A-CREB transgene (Lee et al., 2005, 2009), we limited the duration of SE to 2 h via the injection of diazepam (see Cunha et al. (2009) for a description of the neuroprotective effects of terminating SE with diazepam). With this paradigm, we consistently observed limited cell death in both WT mice and A-CREB transgenic mice at the 2-day post-SE time point (Fig. 6B); of note, this contrasts with the robust cell death observed in Fig. 2C, where SE activity was not terminated. As shown in Fig. 6C, D, NDEL1 expression at 2 days post-SE was significantly reduced in A-CREB transgenic mice compared to wild-type littermates in the GCL (P=0.0043, unpaired two-tailed Student's t-test, t=4.3464, df=6; F test to compare variance did not reveal a significant difference between the two genotypes: P=0.4837, F=1.052, DFn=3, DFd=3), CA1 (P=0.0164, two-tailed Student's t-test, t=3.298, df=6; F test to compare variance did not reveal a significant difference between the two genotypes: P=0.3918, F=1.412, DFn=3, DFd=3), and CA3 (P=0.0018, two-tailed Student's t-test, t=5.3, df=6; F test to compare variance did not reveal a significant difference between the two genotypes: P=0.2299, F=2.564, DFn=3, DFd=3).

Finally, high-magnification confocal microscopy of the CA1 cell layer (Fig. 6E) was used to detect cellular-level suppression of NDEL1 expression. Of note, A-CREB transgenic cells exhibited relatively low NDEL1 expression, whereas marked NDEL1 expression was detected in non-transgenic cells. Together these data indicate that NDEL1 expression is regulated by the CREB/CRE transcriptional pathway in the CNS.

DISCUSSION

Here we provide evidence of broad-based NDEL1 expression in the brain. Further, we show that NDEL1 expression is regulated by neuronal activity, and that this expression is likely to be under the control of the CREB/CRE transcriptional pathway.

As noted above, in the developing CNS, NDEL1 is expressed in immature neurons where it regulates neuronal migration, protein transport and neurite outgrowth (Niethammer et al.,

2000; Sasaki et al., 2000; Toyo-oka et al., 2003; Kamiya et al., 2006). Further, in the mature nervous system, the recent work of Pei et al. (2014) characterized an NDEL1 expression pattern similar to the one described here. Along these lines, marked expression of NDEL1 was observed in cortex and cerebellar cell populations, whereas fairly modest expression was detected within the principal cell layers of the hippocampus.

The upstream signaling events that regulate NDEL1 expression have not been well characterized. However, one clue regarding its regulation was provided by Impey et al. (2004), when they showed that forskolin can increase NDEL1 expression. Forskolin is an adenylate cyclase activator used to increase cAMP, thus raising the prospect that NDEL1 is under the control of the CREB/CRE transcriptional pathway. The CREB/CRE pathway is of particular interest, given its well-characterized role in neuronal development and adaptive plasticity in the CNS (Poser and Storm, 2001; Sakamoto et al., 2011; Kandel, 2012). In line with this, CREB mediates activity-dependent dendritic outgrowth, branching and synapse formation (Gruart et al., 2012; Dhar et al., 2014). Further, numerous genes that are important for cell survival are transcribed via a CREB/CRE-dependent mechanism, including BDNF and Bcl-2 (Wilson et al., 1996; Shieh and Ghosh, 1999; Obrietan et al., 2002).

Here we provide several data sets indicating that NDEL1 expression is regulated by CREB activity. Along these lines, we provide data showing CREB occupancy within the CpG island that is just upstream of the *NDEL1* transcriptional start site. Further, we show that transgenic repression of CREB reduces NDEL1 expression *in vivo*. These data provide solid support for the idea that NDEL1 expression is regulated by the CREB/CRE pathway. Of note, several studies have identified CRE motifs within the promotor region of the *NDEL1* gene. Along these lines Zhang et al. (2005), identified multiple (4) CRE half site upstream of the mouse *NDEL1* gene. Further, CREB ChIP data from mouse neuronal culture were used to identify numerous CREB bindings sites within the 5′ regulatory region of the *NDEL1* gene (Lesiak et al., 2013). Finally, data from the ENCODE consortium used ChIP seq to detect CREB binding near the promoter (and within the CpG island) of the human *NDEL1* gene (Gerstein et al., 2012; Wang et al., 2012, 2013). Thus, the CREB pathway likely provides a clear mechanistic route through which changes in synaptic activity regulate NDEL1 expression in the CNS. Although the functional ramifications of this inducible expression are not clear, one possible effect could be at the level of synapse function and/or formation. Along these lines, the NDEL1 homolog nuclear distribution factor E-homolog 1 (NDE1) was found to be associated with DISC1, and PDE4B at neuronal synapses (Bradshaw et al., 2008). Likewise, disruption of NDEL1 function during development was found to disrupt LIS1 and DISC1 transport to the developing nerve end (Okamoto et al., 2015), and the selective disruption of DISC1/NDEL1 binding was found to affect dendritic development in adult born granule cell neurons (Duan et al., 2007). Together, these data raise the interesting prospect that CREB-regulated NDEL1 expression may play an important role in activity-dependent morphological plasticity in the CNS.

To examine the inducible nature of NDEL1 we profiled its expression using the pilocarpine model of SE. We previously reported that pilocarpine-induced seizures result in CREB phosphorylation and CRE-mediated gene expression (Lee et al., 2007; Hansen et al., 2014). SE also triggers profound alterations in synaptic architecture within the hippocampus,

including the aberrant sprouting of granule cell axons, and CA1 dendrite reorganization (Coulter, 1999; Dudek et al., 2002; Hansen et al., 2014). Hence, given the well-characterized effects that NDEL1 has on neuronal development (including axon extension and growth cone motility) we felt that this model would be an ideal system to examine evoked NDEL1 expression in the mature CNS.

Here we show that SE elicited a robust and lasting increase in NDEL1 expression in the hippocampus. Increased expression was detected in cell processes as well as in the cell bodies in all major cell layers of the hippocampus. In contrast to our findings, a recent study found that pilocarpine stimulated expression of NDEL1 in ectopic blood vessels of the hippocampus but not in the neuronal cell layers (Wu et al., 2014). The reason(s) behind the discord in these findings is not known, although it is worth noting that the referenced study used different post-stimulus time points and younger mice than we used.

In our study, both the acute and lasting increases in NDEL1 expression parallels the expression pattern of other CREB-regulated genes following SE. Along these lines, our prior work showed that over 70 CREB-regulated genes exhibit a similar profile to NDEL1 (Hansen et al., 2014). Further, our work and the work of other labs have shown that there are multiple waves of CRE-mediated transcription induced by SE: from acute induction hours after SE onset, to induction resulting from spontaneous seizure activity (typically occurring many weeks following SE) (Lee et al., 2007; Beaumont et al., 2012; Hansen et al., 2014). As noted above, CREB plays a key role in regulating activity-dependent synaptic plasticity in the mature nervous system, and also is important for neuronal morphogenesis during development. These observations raise the possibility that some of the effects of CREB on neuronal development could be mediated by NDEL1. Further, it is tempting to hypothesize that NDEL1 could contribute to SE-evoked pathophysiological alterations in neuronal cell structure. Additional experiments that allow for the cell-specific and temporally-targeted regulation of NDEL1 would be required to address this question.

Acknowledgments

This work was supported by the National Institutes of Health (Grant code: MH103361, NS045758, NS066345, NS091302) and the National Science Foundation (Grant code: 1354612). The authors have no conflict of interest to declare.

Abbreviations

ChIP	chromatin immunoprecipitation
CREB	cAMP response element-binding protein
DAB	diaminobenzidine
DISC1	disrupted in schizophrenia 1
GCL	granule cell layer
GFP	green fluorescent protein
GFAP	glial fibrillary acidic protein

Hil	hilus
LIS1	lissencephaly 1 protein
NDEL1/NUDEL	Nuclear distribution element-like 1
NF-L	neurofilament light subunit
ML	molecular cell layer
PBS	phosphate-buffered saline
PBST	PBS with 0.1% Triton-X
PCL	pyramidal cell layer
SE	status epilepticus
SO	striatum oriens
SR	stratum radiatum
WT	wildtype

References

Ahn S, Olive M, Aggarwal S, Krylov D, Ginty DD, Vinson C. A dominant-negative inhibitor of CREB reveals that it is a general mediator of stimulus-dependent transcription of c-fos. Mol Cell Biol. 1998; 18:967–977. [PubMed: 9447994]

Beaumont TL, Yao B, Shah A, Kapatos G, Loeb JA. Layerspecific CREB target gene induction in human neocortical epilepsy. J Neurosci. 2012; 32:14389–14401. [PubMed: 23055509]

Bradshaw NJ, Hennah W, Soares DC. NDE1 and NDEL1: twin neurodevelopmental proteins with similar 'nature' but different 'nurture'. Biomol Concepts. 2013; 4:447–464. [PubMed: 24093049]

Bradshaw NJ, Ogawa F, Antolin-Fontes B, Chubb JE, Carlyle BC, Christie S, Claessens A, Porteous DJ, Millar JK. DISC1, PDE4B, and NDE1 at the centrosome and synapse. Biochem Biophys Res Commun. 2008; 377:1091–1096. [PubMed: 18983980]

Chansard M, Hong JH, Park YU, Park SK, Nguyen MD. Ndel1, Nudel (Noodle): flexible in the cell? Cytoskeleton. 2011; 68:540–554. [PubMed: 21948775]

Coulter DA. Chronic epileptogenic cellular alterations in the limbic system after status epilepticus. Epilepsia. 1999; 40(Suppl 1):S23–S33.

Cunha AO, Mortari MR, Liberato JL, dos Santos WF. Neuroprotective effects of diazepam, carbamazepine, phenytoin and ketamine after pilocarpine-induced status epilepticus. Basic Clin Pharmacol Toxicol. 2009; 104:470–477. [PubMed: 19371260]

Dhar M, Zhu M, Impey S, Lambert TJ, Bland T, Karatsoreos IN, Nakazawa T, Appleyard SM, Wayman GA. Leptin induces hippocampal synaptogenesis via CREB-regulated microRNA-132 suppression of p250GAP. Mol Endocrinol. 2014; 28:1073–1087. [PubMed: 24877561]

Duan X, Chang JH, Ge S, Faulkner RL, Kim JY, Kitabatake Y, Liu XB, Yang CH, Jordan JD, Ma DK, Liu CY, Ganesan S, Cheng HJ, Ming GL, Lu B, Song H. Disrupted-In-Schizophrenia 1 regulates integration of newly generated neurons in the adult brain. Cell. 2007; 130:1146–1158. [PubMed: 17825401]

Dudek FE, Hellier JL, Williams PA, Ferraro DJ, Staley KJ. The course of cellular alterations associated with the development of spontaneous seizures after status epilepticus. Prog Brain Res. 2002; 135:53–65. [PubMed: 12143370]

Fujikawa DG, Shinmei SS, Cai B. Seizure-induced neuronal necrosis: implications for programmed cell death mechanisms. Epilepsia. 2000; 41(Suppl 6):S9–S13.

Gardiner-Garden M, Frommer M. CpG islands in vertebrate genomes. J Mol Biol. 1987; 196:261–282. [PubMed: 3656447]

Gerstein MB, Kundaje A, Hariharan M, Landt SG, Yan KK, Cheng C, Mu XJ, Khurana E, Rozowsky J, Alexander R, Min R, Alves P, Abyzov A, Addleman N, Bhardwaj N, Boyle AP, Cayting P, Charos A, Chen DZ, Cheng Y, Clarke D, Eastman C, Euskirchen G, Frietze S, Fu Y, Gertz J, Grubert F, Harmanci A, Jain P, Kasowski M, Lacroute P, Leng J, Lian J, Monahan H, O'Geen H, Ouyang Z, Partridge EC, Patacsil D, Pauli F, Raha D, Ramirez L, Reddy TE, Reed B, Shi M, Slifer T, Wang J, Wu L, Yang X, Yip KY, Zilberman-Schapira G, Batzoglou S, Sidow A, Farnham PJ, Myers RM, Weissman SM, Snyder M. Architecture of the human regulatory network derived from ENCODE data. Nature. 2012; 489:91–100. [PubMed: 22955619]

Gruart A, Benito E, Delgado-García JM, Barco A. Enhanced cAMP response element-binding protein activity increases neuronal excitability, hippocampal long-term potentiation, and classical eyeblink conditioning in alert behaving mice. J Neurosci. 2012; 32:17431–17441. [PubMed: 23197734]

Guo J, Yang Z, Song W, Chen Q, Wang F, Zhang Q, Zhu X. Nudel contributes to microtubule anchoring at the mother centriole and is involved in both dynein-dependent and -independent centrosomal protein assembly. Mol Biol Cell. 2006; 17:680–689. [PubMed: 16291865]

Hansen KF, Sakamoto K, Pelz C, Impey S, Obrietan K. Profiling status epilepticus-induced changes in hippocampal RNA expression using high-throughput RNA sequencing. Sci Rep. 2014; 4:6930. [PubMed: 25373493]

Impey S, McCorkle SR, Cha-Molstad H, Dwyer JM, Yochum GS, Boss JM, McWeeney S, Dunn JJ, Mandel G, Goodman RH. Defining the CREB regulon: a genome-wide analysis of transcription factor regulatory regions. Cell. 2004; 119:1041–1054. [PubMed: 15620361]

Kamiya A, Tomoda T, Chang J, Takaki M, Zhan C, Morita M, Cascio MB, Elashvili S, Koizumi H, Takanezawa Y, Dickerson F, Yolken R, Arai H, Sawa A. DISC1-NDEL1/NUDEL protein interaction, an essential component for neurite outgrowth, is modulated by genetic variations of DISC1. Hum Mol Genet. 2006; 15:3313–3323. [PubMed: 17035248]

Kandel ER. The molecular biology of memory: cAMP, PKA, CRE, CREB-1, CREB-2, and CPEB. Mol Brain. 2012; 5:14. [PubMed: 22583753]

Lam C, Vergnolle MA, Thorpe L, Woodman PG, Allan VJ. Functional interplay between LIS1, NDE1 and NDEL1 in dynein-dependent organelle positioning. J Cell Sci. 2010; 123:202–212. [PubMed: 20048338]

Lambert de Rouvroit C, Goffinet AM. Neuronal migration. Mech Dev. 2001; 105:47–56. [PubMed: 11429281]

Lee B, Butcher GQ, Hoyt KR, Impey S, Obrietan K. Activity-dependent neuroprotection and cAMP response element-binding protein (CREB): kinase coupling, stimulus intensity, and temporal regulation of CREB phosphorylation at serine 133. J Neurosci. 2005; 25:1137–1148. [PubMed: 15689550]

Lee B, Dziema H, Lee KH, Choi YS, Obrietan K. CRE-mediated transcription and COX-2 expression in the pilocarpine model of status epilepticus. Neurobiol Dis. 2007; 25:80–91. [PubMed: 17029965]

Lee B, Cao R, Choi YS, Cho HY, Rhee AD, Hah CK, Hoyt KR, Obrietan K. The CREB/CRE transcriptional pathway: protection against oxidative stress-mediated neuronal cell death. J Neurochem. 2009; 108:1251–1265. [PubMed: 19141071]

Leite JP, Garcia-Cairasco N, Cavalheiro EA. New insights from the use of pilocarpine and kainate models. Epilepsy Res. 2002; 50:93–103. [PubMed: 12151121]

Lesiak A, Pelz C, Ando H, Zhu M, Davare M, Lambert TJ, Hansen KF, Obrietan K, Appleyard SM, Impey S, Wayman GA. A genome-wide screen of CREB occupancy identifies the RhoA inhibitors Par6C and Rnd3 as regulators of BDNF-induced synaptogenesis. PLoS ONE. 2013; 8:e64658. [PubMed: 23762244]

Marioni JC, Mason CE, Mane SM, Stephens M, Gilad Y. RNA-seq: an assessment of technical reproducibility and comparison with gene expression arrays. Genome Res. 2008; 18:1509–1517. [PubMed: 18550803]

Mathern GW, Pretorius JK, Mendoza D, Lozada A, Kornblum HI. Hippocampal AMPA and NMDA mRNA levels correlate with aberrant fascia dentata mossy fiber sprouting in the pilocarpine model of spontaneous limbic epilepsy. J Neurosci Res. 1998; 54:734–753. [PubMed: 9856858]

Mayford M, Bach ME, Huang YY, Wang L, Hawkins RD, Kandel ER. Control of memory formation through regulated expression of a CaMKII transgene. Science. 1996; 274:1678–1683. [PubMed: 8939850]

Moon HM, Youn YH, Pemble H, Yingling J, Wittmann T, Wynshaw-Boris A. LIS1 controls mitosis and mitotic spindle organization via the LIS1-NDEL1-dynein complex. Hum Mol Genet. 2014; 23:449–466. [PubMed: 24030547]

Nguyen MD, Shu T, Sanada K, Lariviere RC, Tseng HC, Park SK, Julien JP, Tsai LH. A NUDEL-dependent mechanism of neurofilament assembly regulates the integrity of CNS neurons. Nat Cell Biol. 2004; 6:595–608. [PubMed: 15208636]

Niethammer M, Smith DS, Ayala R, Peng J, Ko J, Lee MS, Morabito M, Tsai LH. NUDEL is a novel Cdk5 substrate that associates with LIS1 and cytoplasmic dynein. Neuron. 2000; 28:697–711. [PubMed: 11163260]

Obrietan K, Gao XB, van den Pol AN. Excitatory actions of GABA increase BDNF expression via a MAPK-CREB-dependent mechanism-A positive feedback circuit in developing neurons. J Neurophysiol. 2002; 88:1005–1015. [PubMed: 12163549]

Okamoto M, Iguchi T, Hattori T, Matsuzaki S, Koyama Y, Taniguchi M, Komada M, Xie MJ, Yagi H, Shimizu S, Konishi Y, Omi M, Yoshimi T, Tachibana T, Fujieda S, Katayama T, Ito A, Hirotsune S, Tohyama M, Sato M. DBZ regulates cortical cell positioning and neurite development by sustaining the anterograde transport of Lis1 and DISC1 through control of Ndel1 dual-phosphorylation. J Neurosci. 2015; 35:2942–2958. [PubMed: 25698733]

Ozeki Y, Tomoda T, Kleiderlein J, Kamiya A, Bord L, Fujii K, Okawa M, Yamada N, Hatten ME, Snyder SH, Ross CA, Sawa A. Disrupted-in-Schizophrenia-1 (DISC-1): mutant truncation prevents binding to NudE-like (NUDEL) and inhibits neurite outgrowth. Proc Natl Acad Sci. 2003; 100:289–294. [PubMed: 12506198]

Pei Z, Lang B, Fragoso YD, Shearer KD, Zhao L, Mccaffery PJ, Shen S, Ding YQ, McCaig CD, Collinson JM. The expression and roles of Nde1 and Ndel1 in the adult mammalian central nervous system. Neurosci. 2014; 271:119–136.

Poser S, Storm DR. Role of Ca2+-stimulated adenylyl cyclases in LTP and memory formation. Int J Dev Neurosci. 2001; 19:387–394. [PubMed: 11378299]

Sasaki S, Mori D, Toyo-oka K, Chen A, Garrett-Beal L, Muramatsu M, Miyagawa S, Hiraiwa N, Yoshiki A, Wynshaw-Boris A, Hirotsune S. Complete loss of Ndel1 results in neuronal migration defects and early embryonic lethality. Mol Cell Biol. 2005; 25:7812–7827. [PubMed: 16107726]

Sasaki S, Shionoya A, Ishida M, Gambello MJ, Yingling J, Wynshaw-Boris A, Hirotsune S. A LIS1/NUDEL/cytoplasmic dynein heavy chain complex in the developing and adult nervous system. Neuron. 2000; 28:681–696. [PubMed: 11163259]

Sakamoto K, Karelina K, Obrietan K. CREB: a multifaceted regulator of neuronal plasticity and protection. J Neurochem. 2011; 116:1–9. [PubMed: 21044077]

Shieh PB, Ghosh A. Molecular mechanisms underlying activity-dependent regulation of BDNF expression. J Neurobiol. 1999; 41:127–134. [PubMed: 10504200]

Shu T, Ayala R, Nguyen MD, Xie Z, Gleeson JG, Tsai LH. Ndel1 operates in a common pathway with LIS1 and cytoplasmic dynein to regulate cortical neuronal positioning. Neuron. 2004; 44:263–277. [PubMed: 15473966]

Toyo-oka K, Shionoya A, Gambello MJ, Cardoso C, Leventer R, Ward HL, Ayala R, Tsai LH, Dobyns W, Ledbetter D, Hirotsune S, Wynshaw-Boris A. 14-3-3epsilon is important for neuronal migration by binding to NUDEL: a molecular explanation for Miller-Dieker syndrome. Nat Genet. 2003; 34:274–285. [PubMed: 12796778]

Vallee RB, McKenney RJ, Ori-McKenney KM. Multiple modes of cytoplasmic dynein regulation. Nat Cell Biol. 2012; 14:224–230. [PubMed: 22373868]

Vize PD, McCoy KE, Zhou X. Multichannel wholemount fluorescent and fluorescent/chromogenic in situ hybridization in *Xenopus* embryos. Nat Protoc. 2009; 4:975–983. [PubMed: 19498377]

Wang L, Liu YH, Huang YG, Chen LW. Time-course of neuronal death in the mouse pilocarpine model of chronic epilepsy using Fluoro-Jade C staining. Brain Res. 2008; 1241:157–167. [PubMed: 18708038]

Wang J, Zhuang J, Iyer S, Lin X, Whitfield TW, Greven MC, Pierce BG, Dong X, Kundaje A, Cheng Y, Rando OJ, Birney E, Myers RM, Noble WS, Snyder M, Weng Z. Sequence features and chromatin structure around the genomic regions bound by 119 human transcription factors. Genome Res. 2012; 22:1798–1812. [PubMed: 22955990]

Wang J, Zhuang J, Iyer S, Lin XY, Greven MC, Kim BH, Moore J, Pierce BG, Dong X, Virgil D, Birney E, Hung JH, Weng Z. Factorbook.org: a Wiki-based database for transcription factor-binding data generated by the ENCODE consortium. Nucleic Acids Res. 2013; 41(Database issue):D171–D176. [PubMed: 23203885]

Wilson BE, Mochon E, Boxer LM. Induction of bcl-2 expression by phosphorylated CREB proteins during B-cell activation and rescue from apoptosis. Mol Cell Biol. 1996; 16:5546–5556. [PubMed: 8816467]

Wu Q, Li Y, Shu Y, Feng L, Zhou L, Yue ZW, Luo ZH, Wu ZG, Xiao B. NDEL1 was decreased in the CA3 region but increased in the hippocampal blood vessel network during the spontaneous seizure period after pilocarpine-induced status epilepticus. Neurosci. 2014; 268:276–283.

Youn YH, Pramparo T, Hirotsune S, Wynshaw-Boris A. Distinct dose-dependent cortical neuronal migration and neurite extension defects in Lis1 and Ndel1. J Neurosci. 2009; 29:15520–15530. [PubMed: 20007476]

Zhang X, Odom DT, Koo SH, Conkright MD, Canettieri G, Best J, Chen H, Jenner R, Herbolsheimer E, Jacobsen E, Kadam S, Ecker JR, Emerson B, Hogenesch JB, Unterman T, Young RA, Montminy M. Genome-wide analysis of cAMP-response element binding protein occupancy, phosphorylation, and target gene activation in human tissues. Proc Natl Acad Sci USA. 2005; 102:4459–4464. [PubMed: 15753290]

Zhang Q, Wang F, Cao J, Shen Y, Huang Q, Bao L, Zhu X. Nudel promotes axonal lysosome clearance and endo-lysosome formation via dynein-mediated transport. Traffic. 2009; 10:1337–1349. [PubMed: 19522757]

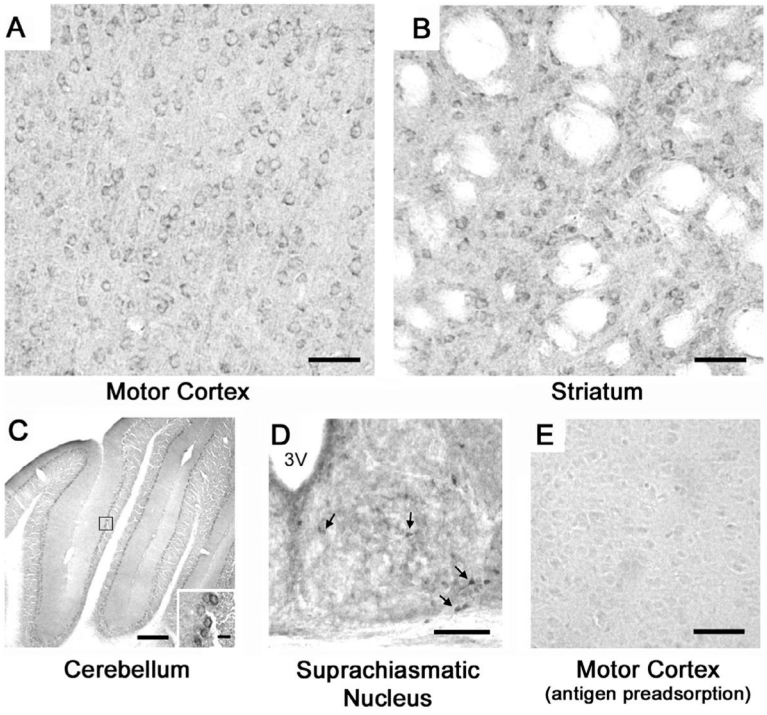

Fig. 1.

NDEL1 expression in the adult mouse brain. Representative immunolabeling for NDEL1 is presented for the motor cortex (A), striatum (B), cerebellum (C) and suprachiasmatic nucleus (D). Note the marked cellular expression within all brain regions. (E) As a control, the NDEL1 antibody was incubated with an NDEL1 peptide, and then tissue from the motor cortex was immunolabeled: note the loss of signal relative to the immunostaining shown in *A*. Arrows in D indicate NDEL1 positive cells in the suprachiasmatic nucleus, and the boxed region in C is magnified as a subpanel. Scale bars=50 μm for A, B and E, 150 μm for C, 10 μm for the high-magnification image in C, and 100 μm for D. Data are representative of 6 animals.

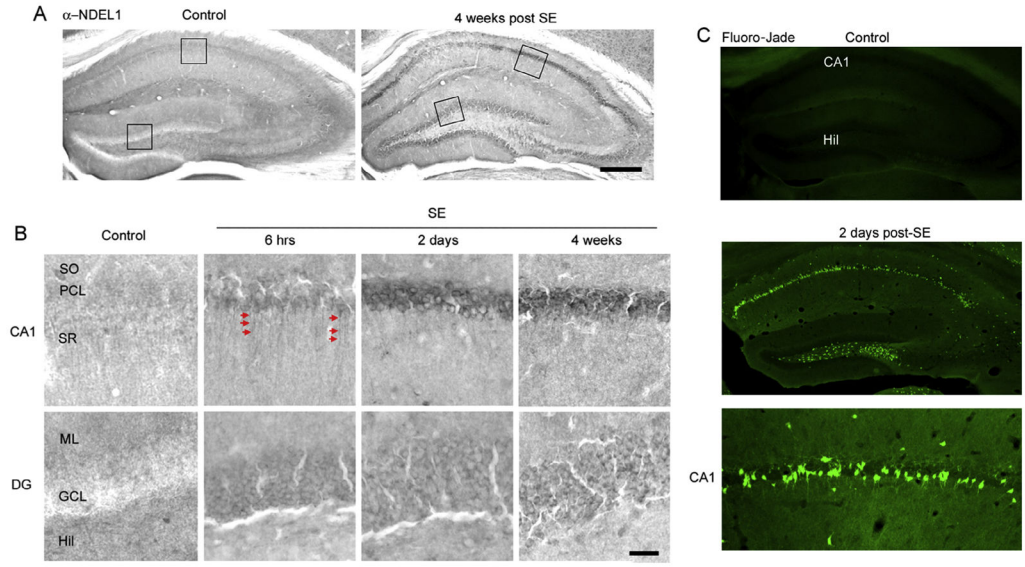

Fig. 2.

Status epilepticus stimulates NDEL1 expression in the hippocampus. (A, B) NDEL1 expression was examined at 3 post-SE time points: 6 h, 2 days and 4 weeks, as well as in vehicle-injected control mice. Relative to control mice, SE evoked a marked increase in NDEL1 expression at each of the three time points. Within the principal excitatory cell layers, NDEL1 upregulation was observed in the cytosol and neuronal processes. Boxed regions in *A* are magnified in *B*, and parallel high-magnification data sets are presented for the 6-h and 2-day time points. SO, striatum oriens; PCL, pyramidal cell layer; SR, stratum radiatum; ML, molecular cell layer; GCL, granule cell layer; Hil, hilus. Arrows in B indicate representative NDEL1-positive processes from CA1 neurons. Scale bars indicate 200 μm in A and 20 μm in B. Data are representative of 6 animals per condition. (C) Representative hippocampal Fluoro-Jade labeling from vehicle-injected mice (top panel: Control) and from animals processed at 2 days post-SE (middle panel). Of note, SE elicited marked cell death in the hilus and CA1 cell layer; a magnified micrograph of the CA1 cell is shown in the bottom panel. Cell death was not detected in control mice. Hil, hilus.

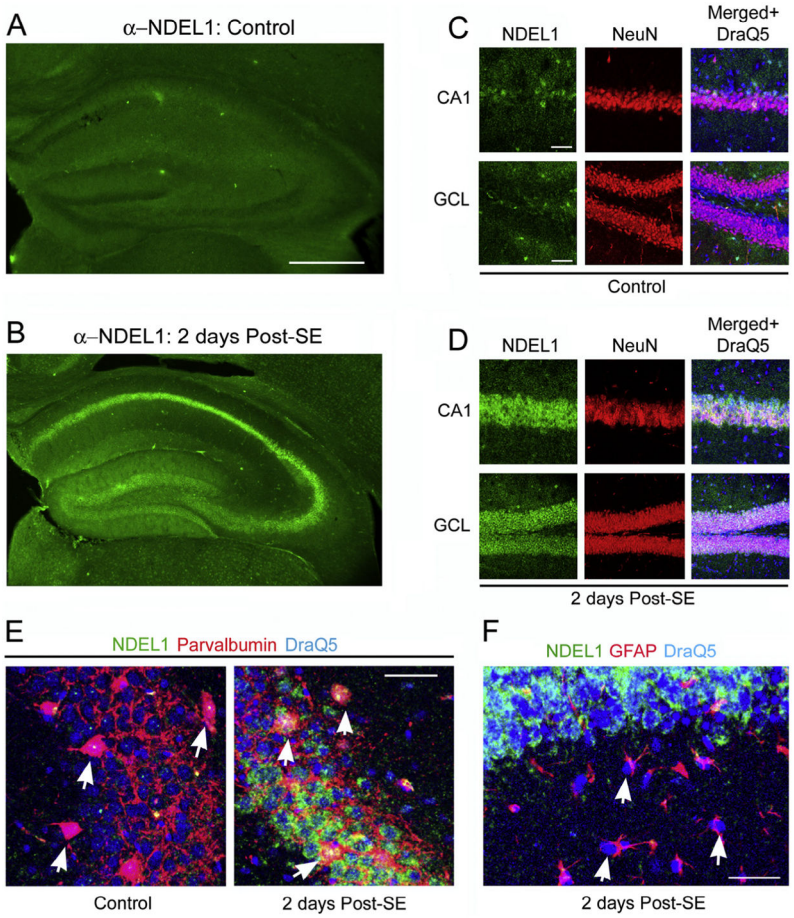

Fig. 3.

Cell-type specific expression of NDEL1 in the hippocampus. (A, B) Representative immunofluorescence images of the hippocampus from a control mouse and a mouse at the 2-day post-SE time point: note the elevated expression of NDEL1 in the principal cell layers at the 2-day time point. Scale bar=300 μm. (C, D). Double immunolabeling for NDEL1 and NeuN confirmed that induction occurs in neuronal cells within the CA1 and GCL. Scale bar=40 μm. (E) Control and 2-day post-SE tissue was processed for NDEL1 and the GABAergic neuronal marker parvalbumin A. Representative data from the CA3/CA2 junction reveals an SE-evoked increase in NDEL1 expression in parvalbumin A-positive cells (Arrows denote the locations of parvalbumin-positive interneurons). For the 2-day time point, the yellow hue of the parvalbumin-positive cells denotes colocalized expression with NDEL1.Scale bar=15 μm. (F) Representative immunolabeling reveals limited NDEL1 expression in GFAP-positive glial cells. Representative data are presented for the 2-day post-SE time point. Scale bar=15 μm. Data are representative of 4 animals per condition. (For interpretation of the references to colour in this figure legend, the reader is referred to the web version of this article.)

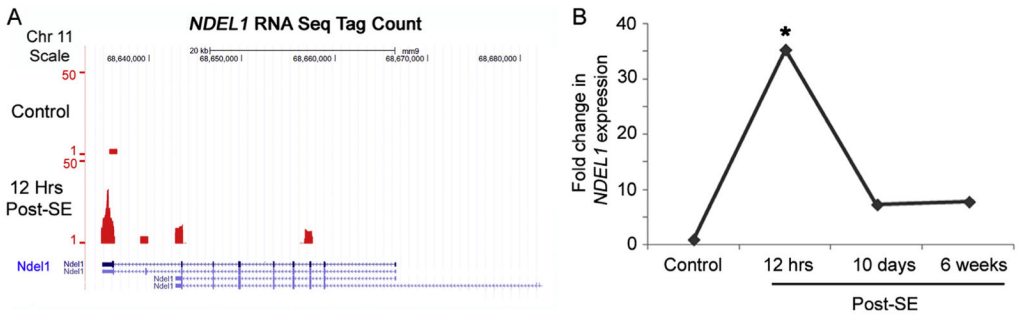

Fig. 4.

Hippocampal NDEL1 expression profiling via RNA seq. (A) RNA seq tag count data from the control condition and the 12-h post-SE time point were loaded on the UCSC genome browser and presented for the *NDEL1* gene located on chromosome 11. Note the relative increase in tag density for the 12-h time point. (B) Fold changes (relative to the control condition) in *NDEL1* expression are presented for the 3 post-SE time points. * denotes a statistically significant increase in NDEL1 expression (q<0.01), relative to the control condition.

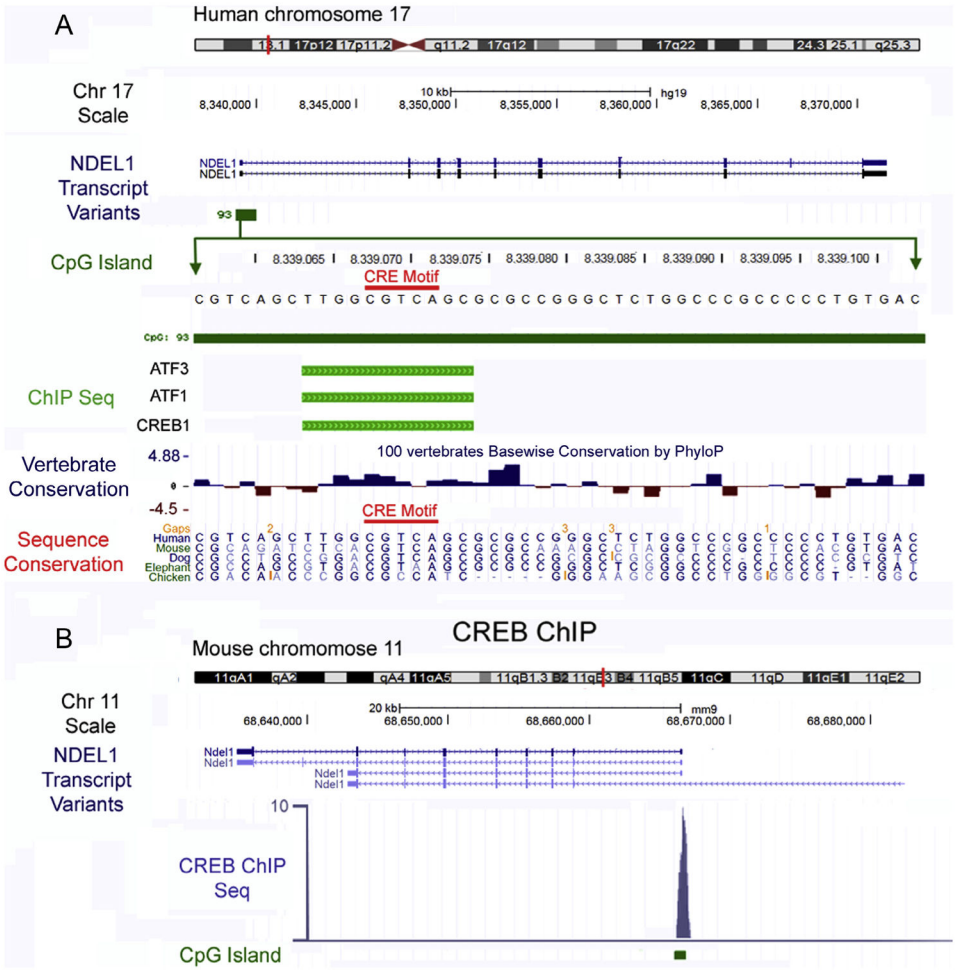

Fig. 5.

The CREB/CRE pathway regulates NDEL1 expression. (A) UCSC genome assembly (mm9) for the human *NDEL1* loci on chromosome 17. A subregion within the CpG island was expanded, and the location of a putative CRE half-site is denoted (CRE motif). ChIP Seq data provided by the Encode Consortium detected ATF3, ATF1 and CREB binding associated with this CRE site. Sequence conservation data are also provided for the expanded region. (B) Murine CREB ChIP Seq data were loaded onto the UCSC genome browser and presented for the mouse *NDEL1* loci located on chromosome 11. Note that the CREB ChIP tag density is located within a CpG island.

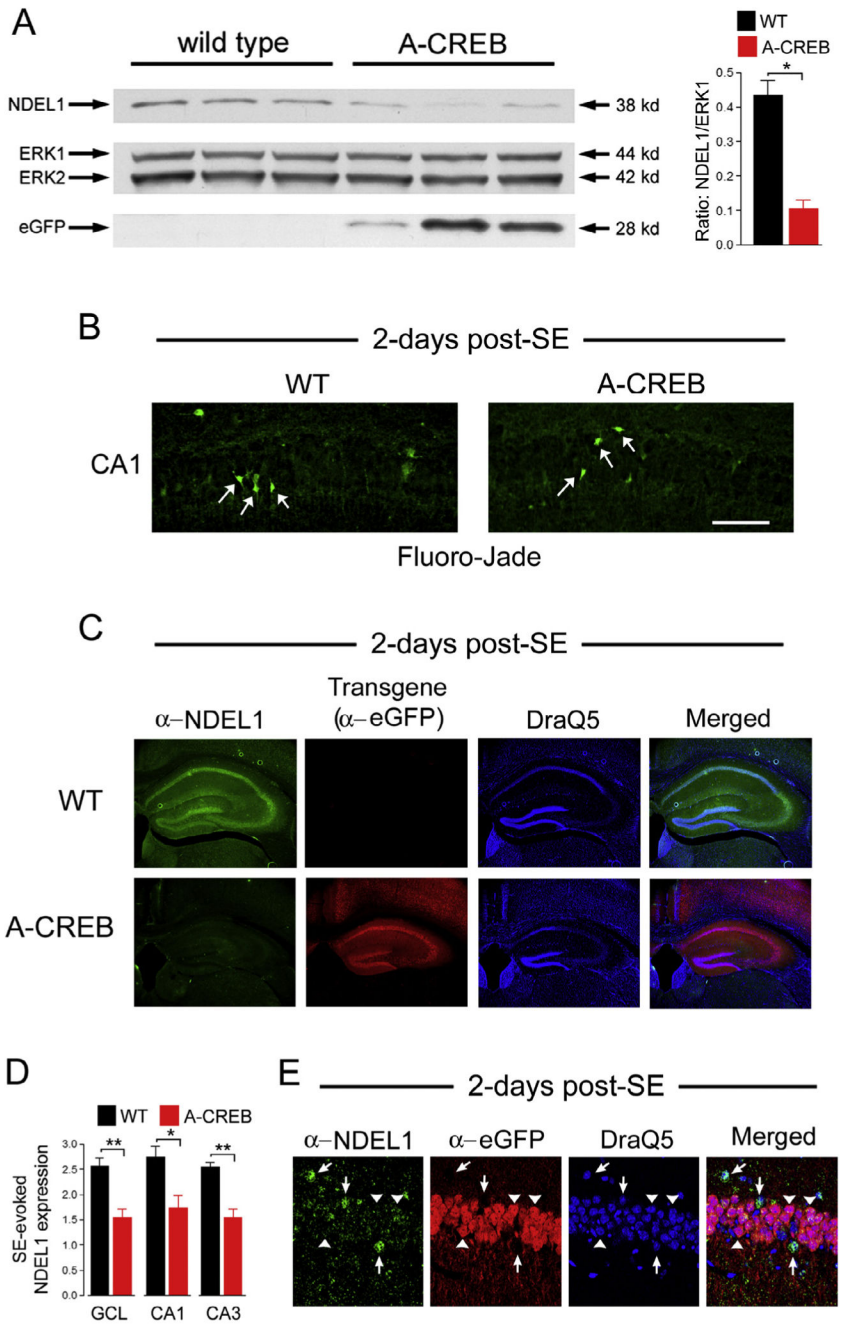

Fig. 6.

The CREB/CRE pathway regulates NDEL1 expression (C) CaMKII-tTA mice were crossed with A-CREB/eGFP-transgenic mice, and NDEL1 expression was profiled under basal conditions and following SE. (A: left panel) Striatal tissue was harvested from A-CREB transgenic mice, and wild-type littermates and profiled for NDEL1 via Western analysis. Relative to wild-type mice, NDEL1 expression was reduced in A-CREB transgene mice. Tissue from three animals was profiled for each genotype. Total ERK expression was used as a loading control, and eGFP was probed to monitor transgene expression. (A: right panel)

Densitometric quantitation of NDEL1 expression in WT and A-CREB transgenic mice. For each lane, NDEL1 expression was divided by ERK1 levels and expressed as the mean ratio for the genotype. $^{*}P<0.05$. (B) Representative Fluoro-Jade labeling within the CA1 cell layer from WT and A-CREB transgenic mice. Of note, the 2-h SE paradigm elicited limited levels of cell death in both mouse lines. Arrows denote a subset of the Fluoro-jade-positive cells. Scale bar=20 μm. (C) NDEL1 expression was profiled via immunofluorescence labeling at 2 days post-SE in WT and A-CREB transgenic mice. Representative hippocampal sections reveal a marked suppression of NDEL1 in A-CREB transgenic mice. Immunolabeling (using the red channel) against the eGFP transgene revealed robust expression throughout the hippocampus of A-CREB mice. (D) Quantitation of SE-evoked NDEL1 expression in the hippocampus of WT and ACREB mice. Data were normalized to NDEL1 expression in the corpus callosum on an animal-by-animal basis. Mean data (+ the SEM) are presented for the major cell layers of the hippocampus. Data were averaged from 4 animals per condition. $^{*}P<0.05$; $^{**}P<0.01$. (E) NDEL1 expression in the CA1 cell layer of A-CREB transgenic mice (2 days post-SE). Of note, in cells with relatively high levels of NDEL1 (denoted by arrows), minimal transgene expression was detected (as assessed via eGFP labeling). However, in cells with high levels of the transgene (denoted with arrowheads), relatively low levels of NDEL1 were detected. (For interpretation of the references to colour in this figure legend, the reader is referred to the web version of this article.)